Europe PMC Funders Group
Author Manuscript
Endocrinology. Author manuscript; available in PMC 2011 March 28.

Published in final edited form as:
Endocrinology. 2009 February ; 150(2): 1000–1013. doi:10.1210/en.2008-0456.

Identification of Novel Trophoblast Invasion-Related Genes: Heme Oxygenase-1 Controls Motility via Peroxisome Proliferator-Activated Receptor γ

Martin Bilban, **Peter Haslinger**, **Johanna Prast**, **Florian Klinglmüller**, **Thomas Woelfel**, **Sandra Haider**, **Alexander Sachs**, **Leo E. Otterbein**, **Gernot Desoye**, **Ursula Hiden**, **Oswald Wagner**, and **Martin Knöfler**

Department of Laboratory Medicine (M.B., F.K., T.W., O.W.), Department of Obstetrics and Fetal-Maternal Medicine, Reproductive Biology Unit (P.H., J.P., S.H., M.K.), Medical University of Vienna, A-1090 Vienna, Austria; Ludwig Boltzmann Institute for Clinical and Experimental Oncology (M.B., F.K., T.W., O.W.), A-1090 Vienna, Austria; Department of Statistics and Probability Theory (F.K., T.W.), University of Technology, A-1040 Vienna, Austria; Department of Surgery (M.B., A.S., L.E.O.), Beth Israel Deaconess Medical Center, Harvard Medical School, Boston, Massachusetts 02215; and Department of Obstetrics and Gynecology (G.D., U.H.), Medical University of Graz, A-8036 Graz, Austria

Abstract

Invasion of cytotrophoblasts (CTBs) into uterine tissues is essential for placental development. To identify molecules regulating trophoblast invasion, mRNA signatures of purified villous (CTB, poor invasiveness) and extravillous trophoblasts (EVTs) (high invasiveness) isolated from first trimester human placentae and villous explant cultures, respectively, were compared using GeneChip analyses yielding 991 invasion/migration-related transcripts. Several genes involved in physiological and pathological cell invasion, including A disintegrin and metalloprotease-12, -19, -28, as well as Spondin-2, were up-regulated in EVTs. Pathway prediction analyses identified several functional modules associated with either the invasive or noninvasive trophoblast phenotype. One of the genes that was down-regulated in the invasive mRNA pool, heme oxygenase-1 (HO-1), was selected for functional analyses. Real-time PCR analyses, Western blotting, and immunofluorescence of first trimester placentae and differentiating villous explant cultures demonstrated down-regulation of HO-1 in invasive EVTs as compared with CTBs. Modulation of HO-1 expression in loss-of as well as gain-of function cell models (BeWo and HTR8/SVneo, respectively) demonstrated an inverse relationship of HO-1 expression with trophoblast migration in transwell and wound healing assays. Importantly, HO-1 expression led to an increase in protein levels and activity of the nuclear hormone receptor peroxisome proliferator activated receptor (PPAR) γ. Pharmacological inhibition of PPARγ abrogated the inhibitory effects of HO-1 on trophoblast migration. Collectively, our results demonstrate that gene expression profiling of EVTs and CTBs can be used to unravel novel regulators of cell invasion. Accordingly, we identify HO-1 as a negative regulator of trophoblast motility acting via up-regulation of PPARγ.

Copyright © 2009 by The Endocrine Society

Address all correspondence and requests for reprints to: Martin Knöfler, Ph.D., Department of Obstetrics and Fetal-Maternal Medicine, Reproductive Biology Unit, Medical University of Vienna, Waehringer Guertel 18-20, A-1090 Vienna, Austria. martin.knoefler@meduniwien.ac.at..

Disclosure Statement: The authors have nothing to disclose.

Europe PMC Funders Author Manuscripts
Europe PMC Funders Author Manuscripts

Europe PMC Funders Author Manuscripts

Europe PMC Funders Author Manuscripts

Invasion of mononuclear cytotrophoblasts (CTBs) into the uterus is a key process of successful human placental and embryonic development. As a result the embryo becomes anchored to the maternal tissue, and stromal compartments as well as uteroplacental vessels will be invaded. Degradation of maternal smooth muscle around maternal spiral arteries and replacement of endothelial cells by endovascular trophoblasts ultimately lead to the dilation of the vessel lumen, which is necessary to enhance intervillous blood flow (1, 2). This particular vascular connection between mother and fetus ensures a continuous supply of nutrients and oxygen during pregnancy. Failures in the particular trophoblast differentiation process are associated with different gestational diseases. Shallow invasion of decidual tissue and incomplete transformation of spiral arteries are hallmarks of maternal preeclampsia, a life-threatening hypertensive disorder of the mother affecting up to 7% of all pregnancies, and of severe intrauterine growth restriction (3, 4).

Although invasive trophoblast differentiation is a physiological process, there are striking similarities between invasive CTBs and invasive cancer cells. During invasion trophoblast cells lose markers of the polarized epithelium, such as $\alpha 6\beta 4$ integrin, transiently down-regulate the adherens junction protein E-cadherin, and induce receptors for fibronectin (FN) and collagens, *i.e.* $\alpha 5\beta 1$ and $\alpha 1\beta 1$ integrins (5, 6). Moreover, cells up-regulate different matrix metalloproteinases and the urokinase plasminogen activator (uPA)/uPA receptor system, thereby promoting matrix degradation and migration (7, 8). Because invasive trophoblasts acquire tumor-like properties, they may undergo a molecular process similar to an epithelial-mesenchymal transition that is thought to play a critical role in cancer cell invasion and metastasis (9). Indeed, one of the critical steps of epithelial-mesenchymal transition, the activation of Wingless (Wnt)-dependent transcription factors of the T-cell factor family through nuclear β-catenin, also takes place in CTBs, thereby promoting Wnt-induced invasion and migration (10). However, in contrast to tumor cell column formation, cell cycle exit and motility of CTBs are tightly controlled by placental and decidual proteins determining time flow and depth of cell invasion (8, 11). For example, local activities of matrix metalloproteinases and uPA are regulated by decidual expression of tissue inhibitors of metalloproteinases and plasminogen activator inhibitors, respectively (12). Despite these facts, signaling pathways and key regulatory transcription factors controlling human trophoblast invasion have not been fully elucidated (13). As a consequence, molecular mechanisms and sequential events leading to the pathogenesis of the gestational diseases remain largely unknown.

To gain more insight into the regulatory mechanisms of trophoblast invasion, here, we investigated whole-genome gene expression profiles of nonmigratory villous CTBs and invasive, extravillous trophoblasts (EVTs) purified from first trimester placentae and differentiating villous explant cultures, respectively. Comparative analyses and gene set enrichment analysis (GSEA) identified several molecular pathways/gene sets associated with either the invasive (extracellular matrix synthesis/remodeling, energy reserve metabolism) or the noninvasive (regulation of stress response, phosphatidylinositol 3-kinase-Akt signaling, chromatin remodeling) differentiation process. One of those genes, heme oxygenase-1 (HO-1), was significantly down-regulated in migratory trophoblasts. HO-1 degrades heme into free iron, carbon monoxide (CO), and biliverdin (14). To date, a putative role of HO-1 in invasive trophoblast differentiation has not been investigated. However, there is evidence for such a function because differential expression of the protein was noticed along trophoblast cell columns (15). To elucidate the role of HO-1 in trophoblasts, descriptive analyses and functional studies using micro-RNA (miRNA)-mediated knockdown as well as Tet-On-induced expression of the enzyme were performed in two distinct trophoblast cell lines. One of the genes that emerged was peroxisome proliferator activated receptor (PPAR) γ. PPARγ is a member of the nuclear hormone receptor superfamily that controls the expression of a large number of genes in a positive or

Europe PMC Funders Author Manuscripts

Europe PMC Funders Author Manuscripts

negative manner depending on the cellular context. PPARγ is also expressed in the placenta where it negatively affects trophoblast invasion and migration (16, 17). Here, up-regulation of HO-1 led to higher levels of PPARγ and decreased trophoblast motility, whereas blocking of PPARγ diminished the inhibitory effect of HO-1. The results indicate that HO-1 controls trophoblast migration via regulation of PPARγ expression, suggesting a novel role of HO-1 in the particular differentiation process.

Materials and Methods

Tissue collection

First trimester placental tissues (n = 22) were obtained after termination of normal pregnancies for psychosocial reasons (7th–10th week of pregnancy) using vacuum suction. The study was approved by the ethical committee of the Medical University of Vienna (Vienna, Austria). All individuals gave informed consent for collection and investigational use of tissues.

Culture of primary villous trophoblast and trophoblastic cell lines

CTBs of first trimester (n = 5) placentae were isolated by enzymatic dispersion, Percoll (5–70%; Pharmacia, Uppsala, Sweden) density gradient centrifugation as described (7, 18). Briefly, villous material was digested with a 0.125% (vol/vol) trypsin solution (GIBCO, Life Technologies, Inc., Paisley, UK). The released cells were loaded on top of a Percoll gradient ranging from 70–10% (vol/vol). After centrifugation, trophoblasts were isolated from the middle layer of the gradient (density of 1.048–1.062 g/ml). Subsequently, cells were immunopurified by depleting contaminating human leukocyte antigen (HLA)-I-positive cells with antihuman HLA-ABC antibody (clone W6/32, 0.2 μg/10^6 cells; Sigma Chemical Co., St. Louis, MO) conjugated to antimouse IgG magnetic beads (Dynal, Oslo, Norway), as previously mentioned (19). Cells were seeded on plastics and routinely checked 12 h after seeding using immunofluorescence with cytokeratin 7 (clone OV-TL 12/30, 8.3 μg/ml; Dako, Glostrup, Denmark) and vimentin antibodies (clone Vim 3B4, 1.2 μg/ml; Dako). Immunopurification removed all nontrophoblastic components as well as EVTs, resulting in cultures with purities higher than 98% as mentioned (20). BeWo choriocarcinoma cells were purchased from the European Collection of Cell Cultures (Salisbury, UK) and were cultivated in Ham F12 (Life Technologies) supplemented with 5% fetal bovine serum (Biochrom, AG, Berlin, Germany) and streptomycin/penicillin (Life Technologies) using standard culture conditions (21). Cytotrophoblastic HTR-8/SVneo cells, exhibiting features of EVTs (22), were routinely cultivated in RPMI 1640 (Life Technologies) supplemented with 5% fetal bovine serum and streptomycin/penicillin.

First trimester villous explant culture

The villous explant culture method followed a standard protocol (6, 23). Dissected mesenchymal villous tissues of early pregnancy (~200 explants per placenta) were arranged radially on 80-μl drops of growth-factor-reduced Matrigel (8 mg/ml; BD, Bedford, MA) in 24-well plates, covered with 50 μl serum-free medium [DMEM-Ham's F12 (Life Technologies) 1:1, supplemented with 100 μg/ml streptomycin/penicillin] and incubated for 4 h at 37 C, 5% CO_2 to allow attachment. Wells were then carefully flooded with 500 μl serum-free medium, incubated at 37 C, 5% CO_2, and subsequent growth characteristics were monitored by light microscopy. After 72 h incubation, tissue sections for immunofluorescence or total RNA pools of EVTs (n = 6) for chip analyses were prepared as described (24). The mechanical isolation procedure (removal of villi) results in generation of pure RNA pools expressing mRNAs specific to EVTs such as α1 integrin, α5 integrin, and HLA-G1.

Europe PMC Funders Author Manuscripts

Europe PMC Funders Author Manuscripts

RNA extraction, cRNA synthesis, and gene expression profiling

Total RNA of CTBs (12 h after seeding) and EVTs isolated from five and six first trimester placentae, respectively, was isolated as described (10, 24). Total RNA was checked for integrity by agarose gel electrophoresis and with the Agilent Bioanalyzer 2100 (Agilent Technologies, Inc., Palo Alto, CA). A total of 5 μg total RNA was then used for GeneChip analysis. Preparation of cRNA, hybridization to human U133A GeneChips (Affymetrix, Inc., Santa Clara, CA), and scanning of the arrays were performed according to the manufacturer's protocols (https://www.affymetrix.com) (25).

Bioinformatic analysis

Robust multi-array average signal extraction, normalization, and filtering (to eliminate genes with extremely low expression) were performed as described (26, 27) (http://www.bioconductor.org/). We identified significant differences between sample groups using a previously described method termed “SAM Analysis” (significance analysis of microarrays) (28). Using this statistical approach, comparisons of gene expression with absolute fold changes of at least 2.0-fold (increase or decrease) were selected at a false discovery rate (FDR) of less than 0.05. Hierarchical clustering was performed using euclidian distance measure and average linkage (http://ep.ebi.ac.uk/EP/EPCLUST/). GSEA (29) is a computational method that determines whether a given set of genes (*e.g.* known pathways, specific areas of the genome, or clusters from a cluster analysis) shows statistically significant differences between two phenotypical states (*i.e.* EVTs *vs.* CTBs). Briefly, the GSEA calculation involves three steps: calculation of an enrichment score (ES), followed by estimation of the significance level of ES, and adjustment for multiple hypothesis testing. We used a publicly available database of gene sets (http://www.chip.org/~ppark/Supplements/PNAS05.html) containing Affymetrix HG-U133A probe set identifiers mapped to pathways from Gene Ontology, Kyoto Encyclopedia of Genes and Genomes (KEGG), BioCarta, BioCyc, and SuperArray to test for enrichment in our trophoblast samples.

Real-time PCR

Total RNA (1 μg) was reverse transcribed into cDNA by Moloney murine leukemia virus enzyme (Promega, Mannheim, Germany) with random hexamers (1 μg/μg total RNA). The reaction mixture was incubated at 37 C for 45 min, followed by 15 min at 45 C and 20 min at 70 C. All PCRs were performed using the SYBR Geen kit (Bio-Rad Laboratories, Inc., Hercules, CA). Primers for selected genes were designed via the Primer3 software (http://frodo.wi.mit.edu/cgi-bin/primer3/primer3_www.cgi) and are listed in Table 1. Using the ABI Prism 7700 sequence detection system (PE Applied Biosystems, Warrington, UK), PCR cycling conditions were as follows: initial denaturation at 95 C for 10 min, followed by 40 cycles at 94 C for 30 sec, 60 C for 15 sec and 72 C for 30 sec, and a 10-min terminal incubation at 72 C. Sequence Detector Software (SDS version 1.6.3; PE Applied Biosystems) was used to extract the PCR data, which were then exported to Excel (Microsoft, Redmond, WA) for further analyses. Data were analyzed according to the $2^{-\Delta\Delta CT}$ method (30). The RNA amount of β-actin was used as an internal control (ctrl).

Construction of transgenic cell lines

Constitutive stable HO-1 knockdown in BeWo cells was generated by transduction with the miRNA adapted retroviral vector LMP (Open Biosystems, Huntsville, AL). miRNA-adapted short hairpin RNA against human HO-1 generated in pSM2 vector (Open Biosystems) was subcloned into the LMP vector with *Xho*I and *Eco*RI (Invitrogen Corp., Carlsbad, CA) restriction enzymes. Confirmation was verified by restriction site analysis and sequencing. To produce murine stem cell virus (MSCV) particles, human embryonic kidney 293FT cells

Europe PMC Funders Author Manuscripts

Europe PMC Funders Author Manuscripts

(Invitrogen) were transiently cotransfected with a vector containing the viral packaging proteins gag and pol, a vector containing env, and either LMP (ctrl) or LMP-miHO1 (LMP containing miRNA against human HO-1). Vectors containing gag, env, and pol were kind gifts from Dr. Ewan Rosen (Beth Israel Deaconess Medical Center, Harvard Medical School, Boston, MA). Lipofectamine 2000 (Invitrogen) reagent was used for transfection. Forty-eight hours after transfection, viral supernatants were collected, centrifuged at 1500 rpm for 3 min, filtered through a 0.4-μm filter, supplemented with 8 μg/ml Polybrene (Sigma Chemical), and used to infect BeWo cells. Stable integrants were selected with puromycin (5 μg/ml) over a period of 2 wk. HO-1 knockdown was verified by Western blotting (See Fig. 5B). The coding region of human HO-1 cDNA (a gift of Dr. Matthias Mayerhofer, Department of Laboratory Medicine, Medical University of Vienna, Vienna, Austria) was inserted into the Tet-responsive murine stem cell retroviral vector pRevTRE-hygro (Clontech Laboratories, Inc., Mountain View, CA) at the *Bam*HI and *Hin*-dIII sites within the MCS generating pRevTRE-hHO1. The sc-rttaM2 gene cloned into the vector pMSCV-puro (Clontech Laboratories) was a kind gift of Dr. Nick Houstis (The Broad Institute, Massachusetts Institute of Technology, Cambridge, MA). To produce MSCV retrovirus, human embryonic kidney 293FT cells were transiently cotransfected with a vector containing the viral packaging proteins gag and pol, a vector containing env and pMSCV-scrttaM2puro or pRevTRE-hHO1. Vectors containing gag, env, and pol were kind gifts from Dr. Ewan Rosen. Lipofectamine 2000 reagent was used for transfection. Forty-eight hours after transfection, viral supernatants were collected, centrifuged at 1500 rpm for 3 min, filtered through a 0.4-μm filter, supplemented with 8 μg/ml Polybrene, and used to infect HTR-8/SVneo cells. The Tet-On system was introduced in two steps. First, the construct that drives expression of the tetracycline-sensitive transcription factor, sc-rttaM2, was integrated and selected with puromycin (5 μg/ml; Sigma Chemical). Second, the construct containing a tetracycline-response element that drives expression of HO-1 was integrated and selected with hygromycin (0.175 mg/ml; Sigma Chemical). Stable cell pools transduced with either empty plasmid or pRevTRE-hHO1 were termed HTR8 and HTR8-HO1, respectively. Inducible HO-1 expression was verified by Western blotting. Two to three rounds of hygromycin selection resulted in almost 100% enrichment of HO-1 expressing cells, as demonstrated by Western blotting and immunofluorescence staining after doxycycline (DOX) (1 μg/ml; Sigma Chemical) treatment (See Fig. 5, D and E).

Western blot analyses

Western blot analyses were performed using standard protocols as recently done (10, 31). Equal amounts of protein lysates (35 μg) were separated on 10% sodium dodecyl sulfate/polyacrylamide gels and transferred onto polyvinylidene fluoride membranes (GE Healthcare, Amersham, Buckinghamshire, UK). After blocking, filters were incubated overnight (4 C) with monoclonal mouse antibodies against human HO-1 (1:1000; Stressgen, Ann Arbor, MI), PPARγ (1:500; Santa Cruz Biotechnology, Inc., Santa Cruz, CA), and β-actin (1:5000; Abcam, Inc., Cambridge, MA). After 1 h treatment (room temperature) with secondary antibodies (antimouse Ig horseradish peroxidase linked, 1:50,000; Amersham), signals were developed using the ECL Plus Western Blotting Detection System (Amersham Pharmacia Biotech, Uppsala, Sweden).

Immunofluorescence

Cells grown on coverslips were washed, fixed with 4% paraformaldehyde, permeabilized with 0.5% Triton X-100, and blocked with goat serum. Expression of HO-1 was detected with the antibody described previously. Cells were incubated with secondary antibodies conjugated to Alexa488 (1:500; Molecular Probes, Inc., Eugene, OR), and visualized using a Zeiss Axioskop 2 microscope (Carl Zeiss MicroImaging, Inc., Thornwood, NY), Zeiss Axiocam, and Photoshop (Adobe Systems, Inc., San Jose, CA). As a negative ctrl,

Europe PMC Funders Author Manuscripts

Europe PMC Funders Author Manuscripts

coverslips were incubated with the secondary antibodies alone (data not shown). First trimester villous ex-plant cultures (n = 3) and first trimester placental tissue (n = 5) were fixed, snap frozen, and 3 μm serial cryosections were performed as recently described (19, 24). Slides were incubated overnight with primary antibody, washed three times in PBS (each 5 min), followed by 5 μg/ml fluorescein isothiocyanate-conjugated goat antimouse or 5 μg/ml goat antirabbit antibodies (1 h; Molecular Probes). The following primary antibodies/dilutions were used: cytokeratin 7 (clone OV-TL, 8.3 μg/ml); vimentin (clone Vim 3B4, 1.2 μg/ml); HLA-G1 (clone MEM-G/1, 50 μg/ml; Exbio, Praha, Czech Republic); HO-1 (clone OSA-110, 1:1000; Stressgen); integrin α1 (clone JBS5, 10 μg/ml; CHEMICON International, Inc., Temecula, CA); integrin α6 (clone 4F10, 5 μg/ml; CHEMICON International); Ki67 (clone Ki-S5, 10 μg/ml; CHEMICON International); and Kip2/p57 (C-20, rabbit, 2 μg/ml; Santa Cruz Biotechnology). As a negative ctrl, the primary antibody was replaced by buffer or isotype IgG. Finally, all sections were counterstained with 1 μg/ml 4′,6-diamidino-2-phenylindole (DAPI) (Roche Diagnostics, Mannheim, Germany) and covered with Fluoromount-G (SouthernBiotech, Birmingham, AL).

Migration assays

Transwell migration assays (8 μm pore size; Corning, Lowell, MA) through filters coated with 10 μg/ml FN (Sigma Chemical) were performed as described (25). After initial experiments to determine the temporal kinetics of migration, subsequent migration assays were performed with 20,000 cells (LMP or miHO1 BeWo) per well for 5 h. HTR8 and HTR8-HO-1 cells were treated with DOX (1 μg/ml) for 24 h, trypsinized, and seeded into the upper wells of transwell filters. DOX (1 μg/ml) was added to the upper and lower wells. For investigation of the role of PPARγ, cells were pretreated with 3 μM GW9662 (Calbiochem, Nottingham, UK) or vehicle (dimethyl sulfoxide; ctrl) for 4 h before migration assays and treated thereafter for the duration of the migration assay. Cells that had migrated through the filters were fixed and stained with crystal violet. The uncoated, upper side of each filter was wiped with a cotton swab to remove cells that had not migrated through the filter. Duplicate filters of each condition were viewed under bright-field optics. Each of eight fields was counted under the light microscope, and the mean number of cells counted per field was determined. Wound healing assays were performed in 24-well plates coated with 10μg/ml FN in PBS. HTR8 and HTR8-HO-1 cells (6×10^5 per well) were seeded and incubated at 37 C for 36 h in the presence of DOX (1 μg/ml). Cell layers were then wounded with a plastic pipette tip and washed three times with serum-free culture medium. The denuded surfaces were recoated with 10 μg/ml FN in serum-free culture medium for 1 h at 37 C. After washing, cells were incubated for an additional 8 h at 37 C using complete culture medium (containing DOX, 1 μg/ml). Digital photographs within each wound were taken before and 8 h after addition of complete medium.

Transient transfection and luciferase reporter assay

Cells were cotransfected in 24-wells with 0.95 μg PPAR-responsive reporter plasmid p(AOX)3-TKSL and 50 ng Renilla luciferase ctrl plasmid (ph-RL; Promega) using Lipofectamine 2000 (according to the manufacturer's instructions) as described previously (36). Twenty-four hours later, protein extracts were assessed for luciferase activity (Promega Corp., Madison, WI) using a luminometer (Lumat LB 9507; EG&G Berthold, Bad Wildbad, Germany). Firefly luminescence values were normalized to Renilla luminescence levels.

Statistical analysis

Migration indices and real-time PCR levels were analyzed using one-way ANOVA, followed by the Tukey test. Because data were not normally distributed, the Mann-Whitney rank sum test was used to determine the level of significance of differences in pairs of various treatment groups. $P < 0.05$ was considered significant.

Europe PMC Funders Author Manuscripts

Europe PMC Funders Author Manuscripts

Results

Gene expression profiling of trophoblast cells with distinct invasive properties

To identify genes potentially regulating cell invasion, trophoblast cells of early human gestation with distinct invasive properties were profiled (Fig. 1). A schematic picture of the localization of the different trophoblast subtypes is presented in Fig. 1A. Distinct gene expression signatures of highly invasive EVTs and poorly invasive CTBs isolated from 11 different first trimester placentae (n = 6 for EVT and n = 5 for CTB) were determined using Affymetrix U133A GeneChips interrogating more than 20,000 genes. To analyze if our cell pools are enriched with cells of distinct invasiveness, we investigated gene expression changes of well-known markers of the epithelial-mesenchymal switch discriminating EVTs from CTBs *in vivo*. The acquisition of an invasive phenotype *in vivo* as well as *in vitro* is characterized by the loss of integrin α6 and gain of integrin $\alpha 5\beta 1$, HLA-G1, and Kip2/p57 staining, as evidenced by immunofluorescence of first trimester villous explant cultures seeded on Matrigel (Fig. 1B) (5, 32). Our GeneChip data successfully parallel these changes at the mRNA level (Fig. 1C). The calculation of SAM led to a scatter plot of the observed relative difference d(I) *vs.* the expected relative difference dE (I) (Fig. 2A). At a Δ value of 0.30, illustrated by the broken lines, 991 genes were considered to be differentially expressed more than or equal to 2.0/less than or equal to 2.0-fold (370 induced and 621 repressed in EVTs compared with CTBs; supplemental Table 1, which is published as supplemental data on The Endocrine Society's Journals Online web site at http://endo.endojournals.org). The full gene lists of EVTs and CTBs are available at Gene Expression Omnibus (http://www.ncbi.nlm.nih.gov/geo/query/acc.cgi?acc=GSE9773). Table 2 summarizes the top 50 differentially expressed genes between EVTs and CTBs. Among the top 50 differentially expressed mRNAs, we found several genes previously reported to regulate cell adhesion/motility (Fig. 2B and Table 2). Indeed, real-time PCR of selected genes demonstrates elevated expression of A disintegrin and metalloprotease (ADAM) 12, 19, 28, Spondin-2, and nidogen-1 but down-regulation of villin-2, Nedd-9, and HO-1 in EVTs, thereby confirming the Gene-Chip data (Table 1).

Pathway prediction analyses

Having defined the expression profiles for EVTs and CTBs, the next challenge was to interpret them objectively. Using GSEA we analyzed whether previously characterized, coregulated sets of genes were more enriched in EVT or CTB cells (GSEA) (26, 29). Tables 3 and 4 display the top 30 pathways enriched in either EVTs or CTBs, respectively. Among others, EVTs were significantly enriched in pathways regulating extracellular matrix synthesis and remodeling, cell adhesion, as well as carbohydrate metabolism. A more detailed analysis of these pathways revealed enhanced expression of several collagen or laminin isoforms, the predominant matrix proteins in the endometrium (33), in addition to Spondin-2, nidogen-1, and several ADAMs (Fig. 3A, Table 3, and supplemental Fig. 1A). These observations suggest that EVT cells may secrete substrates relevant to cell invasion as well as their degrading enzymes. In addition, EVT cells expressed higher levels of enzymes regulating carbohydrate metabolism, including several isoforms of lactate dehydrogenase, aldehyde dehydrogenase, and phosphofructokinase (supplemental Fig. 1B). CTBs were significantly enriched in genes implicated in stress response, signal transduction, and gene regulation, among others (Fig. 3B, Table 4, and supplemental Fig. 2, A and B). A more detailed inspection of these pathways revealed increased expression of genes regulating the response to heavy metals, UV light, oxygen species, and DNA damaging agents, including SOD2, HO-1 (HMOX1), and several heat shock proteins (Fig. 3B). Furthermore, several signal transduction pathways are modulated, including glucocorticoid-, cAMP/Ca^{2+}-, and G protein-coupled receptor signaling (Fig. 3B and Table 4). Interestingly, CTBs display

Europe PMC Funders Author Manuscripts

Europe PMC Funders Author Manuscripts

enhanced expression of a large group of gene sets regulating the nuclear import/export and translation factor activity (supplemental Fig. 2B, *right panel*, and Table 4).

HO-1 expression in first trimester placenta and villous explant cultures

To initiate functional analyses of differentially expressed genes, here, we focused on HO-1, a stress-responsive gene that was recently shown to affect cell migration (34). GeneChip as well as real-time PCR data demonstrate HO-1 mRNA to be suppressed by 2.63- and 3.33-fold, respectively, in invasive EVTs compared with CTBs (Fig. 4A and Table 1). Immunofluorescence of first trimester placentae revealed that HO-1 protein was strongly expressed in proliferative, Ki67-positive CTBs of cell columns, but largely absent from nonproliferating, Kip2/p57-positive EVTs (Fig. 4B). Resembling the *in vivo* HO-1 protein expression, HO-1 staining was strong in cycling CTBs of first trimester explant cultures but decreased in the distal, invasive EVTs (Fig. 4C). To describe more quantitatively the differential HO-1 expression, we also performed Western blotting of isolated primary cultures demonstrating higher levels of HO-1 in CTBs compared with EVTs (Fig. 4D).

HO-1 expression regulates trophoblast motility

To investigate whether HO-1 expression regulates trophoblast migration, we took a two-pronged approach using a loss-of as well as a gain-of function cell model. We knocked down endogenous HO-1 in BeWo cells using retroviral transduction with a miRNA adapted retroviral vector targeting human HO-1 sequence (“miHO1”; Fig. 5A). Using Western blotting we observed an efficient knockdown of HO-1 expression in BeWo cells stably expressing miHO1 (thus called “miHO1”) compared with BeWo cells stably expressing the LMP ctrl sequence (termed “LMP”) (Fig. 5B). To test whether the loss of HO-1 impacts cell motility, LMP and miHO1 cells were subjected to a transwell migration assay. Compared with ctrls (LMP), cell migration toward FN was increased by 70% in cells lacking HO-1 (Fig. 5C). To substantiate this result, we established a DOX-inducible, HO-1-expressing HTR-8/SVneo cell line by retroviral gene transfer and performed similar functional assays. HO-1 protein expression was strongly induced 24 h after DOX addition using Western blotting (Fig. 5D) and immunocytochemistry (Fig. 5E). In transwell assays, mock-transduced cells showed significant migration through FN-coated transwells (Fig. 5E). In contrast, when HO-1 was DOX induced 24 h before and during the migration assay, cell motility was reduced by 37% (Fig. 5F). Similarly, in wound healing assays, trophoblast migration into the denuded area was diminished upon induction of HO-1 (Fig. 5G). HO-1 did not alter cell proliferation in the time frame of migration and wound healing assay. However, 24 h after seeding increased proliferation (118.5% compared with ctrls, 100%; $P = 0.017$) was noticed in HTR-8 cells expressing HO-1. Recently, we demonstrated up-regulation of PPARγ expression by CO, a product of HO-1 enzymatic activity in macrophages (35).

Because activation of PPARγ inhibits trophoblast invasion (16), we asked if the inhibitory effects of HO-1 could be mediated through PPARγ. Noteworthy, CTBs express higher levels of PPARγ than EVTs (Fig. 4D). Our hypothesis was supported by experiments showing that down-regulation of HO-1 expression in miHO1 BeWo cells also decreased PPARγ protein levels (Fig. 6A). Furthermore, HO-1 knockdown in miHO1 BeWo cells reduced expression of a luciferase reporter driven by the PPARγ-dependent promoter (Fig. 6B). Indeed, pharmacological blocking of PPARγ abolished the suppressive effect of HO-1 on migration observed in LMP cells in the absence of GW9662 (Fig. 6E). Similar effects could be detected in HTR8/HO-1 gain-of function cells: induction of HO-1 by DOX for 48 h resulted in higher PPARγ protein levels as well as PPARγ luciferase reporter activity in HTR8-HO1 cells compared with HTR8 ctrl cells (Fig. 6, C and D). Blocking of PPARγ in DOX-treated HTR8 cells with GW9662 added before transwell assays did not significantly

alter trophoblast migration (Fig. 6F). However, blocking of PPARγ in DOX-treated HTR8-HO1 cells reversed the motility inhibiting effect obtained through HO-1/PPARγ overexpression.

Discussion

During the establishment of the human placenta, a highly migratory subpopulation of EVTs, originating from anchoring chorionic villi, invades maternal uterine stroma and blood vessels. Placental research over the past decades has underlined the striking similarities among the mitotic, migratory, and invasive properties of trophoblasts and those of cancer cells, which are known to override mechanisms controlling cellular proliferation, invasion, and death. Therefore, characterization of the complete human transcriptome of different trophoblast subsets by gene expression profiling is well suited to identify critical genes potentially involved in normal and pathological invasion processes. Previously, we have identified putative regulators of trophoblast differentiation by comparing gene expression profiles of trophoblast cells isolated from first and term trimester human placenta (25). In the present paper, we aimed to capture more accurately the distinct molecular signatures of highly and poorly invasive trophoblasts by applying gene expression profiling of purified EVTs and CTBs of first trimester pregnancies. Differential expression of integrins α6, α1, β4, E-cadherin, as well as of HLA-G1 in EVTs and CTBs indicated that the RNA pools correctly represent the respective trophoblast subtypes. So far, several of the most strongly regulated genes, such as extracellular matrix components (nidogen-1, Spondin-2, villin) and remodeling proteases (ADAM-12, -19, -28), were not known to be expressed differentially in invasive and noninvasive trophoblast cells. Because those molecules have known roles in cancer invasion, a role of such genes in trophoblast invasion seems plausible. Although it is not within the scope of this paper to analyze exhaustively the entire database of differentially expressed genes, this study resulted in a very rich data set, which is now provided as a public source. As anticipated, GSEA identified several gene sets implying transition from a sessile to a motile phenotype. Different collagens and matrix-degrading proteases were found to be predominantly expressed in invasive trophoblasts. This may implicate changes in cell adhesion/motility, cell-matrix interaction, and cell signal transduction during invasive trophoblast differentiation. Furthermore, GSEA showed that CTBs and EVTs have widespread differences in other biological processes, including response to stress, carbohydrate metabolism, signal transduction, and gene regulation.

Recent studies demonstrated the importance of HO-1/CO in pregnancy through modulation (*i.e.* reduction) of placental per-fusion pressure by HO-1/CO on the maternal endothelium (15, 36-38). This finding has important consequences with regard to pregnancy specific diseases such as preeclampsia, a hypertensive disorder (38). In this study we highlight a further possible role of HO-1 in the regulation of trophoblast invasiveness. Our immunostainings indicate high expression of HO-1 in proliferative, Ki67-positive cell columns, whereas protein levels were low in noncycling, Ki67-negative, invasive EVTs. This result somewhat contrasts to the one reported previously showing similar or decreased expression in cell column *vs.* EVT (15). We explain this discrepancy based on the fact that the polyclonal anti-HO-1 antibody used by Lyall *et al.* (15) stains nonspecifically as reported elsewhere (39). In addition, in the study by Lyall *et al.* (15) cell columns of midgestation placentae was not analyzed for proliferative status using for example Ki67 antibodies. Assuming that nonproliferating columns with low HO-1 expression were analyzed, it may well be that the decrease in HO-1 gene expression upon invasion could not be easily detected. Therefore, we believe that the HO-1 staining described in this study reflects more accurately the subcellular localization of HO-1. Similar to the HO-1 staining in the early placenta, analyses of first trimester villous explant cultures revealed that HO-1 staining was intense in proximal trophoblast cells (representing CTBs) in contrast to distally, invasive

Europe PMC Funders Author Manuscripts
Europe PMC Funders Author Manuscripts

Europe PMC Funders Author Manuscripts

Europe PMC Funders Author Manuscripts

trophoblast (representing EVTs). The immunohistochemical staining pattern was also confirmed by Western blotting showing decreased HO-1 protein expression in isolated EVT compared with CTBs. Therefore, we analyzed whether the loss of HO-1 expression (in BeWo cells) as well as induction of HO-1 expression (in HTR-8/SVneo cells) may affect cell motility. BeWo trophoblast cells endogenously express HO-1, whereas HTR8/SVneo cells lack HO-1 expression, which could be another feature of their EVT-like phenotype (22). The loss of HO-1 in BeWo cells resulted in increased cell motility. Similarly, DOX-dependent expression of HO-1 revealed an inhibitory effect of the enzyme on HTR-8/SVneo trophoblast motility using transwell as well as wound healing migration assays. Therefore, we conclude that down-regulation of HO-1 in EVT could be a critical step in successful trophoblast invasion. The suppressive effects of HO-1 on trophoblast migration were PPARγ dependent. Up-regulation of PPARγ protein and activity by HO-1 was required to down-regulate cell motility because blocking of PPARγ largely abolished the effect of HO-1 overexpression. Similarly, the increase in cell motility upon knockdown of HO-1 could not be observed in PPARγ-inhibited cells. The exact mechanism by which HO-1 up-regulates PPARγ remains to be elucidated, however, several scenarios may be envisioned that also emphasize a potential role of the enzymatic products of HO-1: 1) a role of CO in up-regulation of PPARγ may be envisioned because it was shown recently by others and us that CO up-regulates PPARγ and PPARδ in macrophages and C2C12 myoblast cells (35, 40); 2) Schild *et al.* (41) previously documented the involvement of p38 MAPK because pharmacological inhibition of p38 led to reduced PPARγ protein expression in term trophoblast cells; 3) epigenetic mechanisms through HO-1 acting as a transcription factor (42); and 4) decreased degradation of PPARγ (43) or differential regulation of scaffold regulatory corepressor or coactivator proteins such as prostaglandin C-1, nuclear hormone receptor corepressor and silencing mediator for retinoid and thyroid hormone receptors, phosphorylation by MAPKs (41, 44), or small ubiquitin-like modifier-ylation (45). Interestingly, addition of GW9662 did not affect cell migration in miHO-1 BeWo knockdown cells and HTR-8 ctrl cells. Therefore, failure of the PPARγ inhibitor to provoke effects on cell migration was only observed in cells expressing low amounts of PPARγ. We hypothesize that the PPARγ dosage could be critical for the migratory response: in miHO-1 BeWo cells, treatment with GW9662 may not increase migration because PPARγ could have decreased below a critical expression level. Conversely, inhibition of HTR-8 ctrls with GW9662 did not increase basal migration because low levels of PPARγ in these cells may not be effective. However, HO-1 may also partly suppress trophoblast migration by mechanisms independent of PPARγ because reversal by the selective PPARγ inhibitor was not complete. Theoretical possibilities include modulation of migration/adhesion molecule expression, including vasodilator-stimulated phosphoprotein (34), integrin $\alpha 5\beta 1$ (46) E-selectin, vascular cell adhesion molecule-1 (47), intercellular adhesion molecule-1 (48), or integrin $\beta 2$ (49). In addition, physical association and/or post-translational modification of the actin cytoskeleton or Akt by HO-1 may contribute to the inhibitory effect on cell migration (50, 51). It is well known that activation of PPARγ inhibits trophoblast invasion either through up-regulation or transrepression of molecules regulating cell invasion (16). Those molecules include the metalloproteinase pregnancy associated plasma protein-A (52), human chorionic gonadotrophin (53), Muc1 (54), leptin, TNFα, IL-1β, TGF$\beta 2$, and placental GH (16). Because some of those molecules (IL-1β, TNFα) are also regulated by HO-1 (14), we speculate that a possible signaling cascade, including HO-1 upstream of PPARγ, may regulate expression of these molecules thereby ultimately controlling trophoblast migration.

In conclusion, the present work delineates mRNA signatures and gene sets of noninvasive and motile trophoblasts providing further options for detailed analyses of the invasive trophoblast differentiation process. Moreover, functional analyses of HO-1, which has been

identified by the comparative gene profiling strategy, indicate that the enzyme could be a critical regulator of trophoblast motility.

Acknowledgments

We thank Eva Muzik for assistance with GeneChip experiments and Martin Posch for critical comments regarding bioinformatic analysis. We also thank the Julie Henry Fund at the Transplant Center of the Beth Israel Deaconess Medical Center, Boston, MA, for its support.

This work was supported by Grant 10239 from the Austrian National Bank, fellowship no. J2626 from the Austrian Science Fund (to M.B.), and Grant P-17894-B14 of the Austrian Science Fund (to M.K.).

Abbreviations

ADAM	A disintegrin and metalloprotease
CO	carbon monoxide
CTB	cytotrophoblast
ctrl	control
DAPI	4′,6-diamidino-2-phenylindole
DOX	doxycycline
ES	enrichment score
EVT	extravillous trophoblast
FDR	false discovery rate
FN	fibronectin
GSEA	gene set enrichment analysis
HLA	human leukocyte antigen
HO-1	heme oxygenase-1
KEGG	Kyoto Encyclopedia of Genes and Genomes
miRNA	micro-RNA
MSCV	murine stem cell virus
PPAR	peroxisome proliferator activated receptor
SAM	significance analysis of microarrays
uPA	urokinase plasminogen activator
Wnt	Wingless

References

1. Harris LK, Keogh RJ, Wareing M, Baker PN, Cartwright JE, Aplin JD, Whitley GS. Invasive trophoblasts stimulate vascular smooth muscle cell apoptosis by a fas ligand-dependent mechanism. Am J Pathol. 2006; 169:1863–1874. [PubMed: 17071607]
2. Pijnenborg R, Bland JM, Robertson WB, Brosens I. Uteroplacental arterial changes related to interstitial trophoblast migration in early human pregnancy. Placenta. 1983; 4:397–413. [PubMed: 6634666]
3. Khong TY, De Wolf F, Robertson WB, Brosens I. Inadequate maternal vascular response to placentation in pregnancies complicated by pre-eclampsia and by small-for-gestational age infants. Br J Obstet Gynaecol. 1986; 93:1049–1059. [PubMed: 3790464]

Europe PMC Funders Author Manuscripts
Europe PMC Funders Author Manuscripts

Europe PMC Funders Author Manuscripts

Europe PMC Funders Author Manuscripts

4. Zhou Y, Damsky CH, Fisher SJ. Preeclampsia is associated with failure of human cytotrophoblasts to mimic a vascular adhesion phenotype. One cause of defective endovascular invasion in this syndrome? J Clin Invest. 1997; 99:2152–2164. [PubMed: 9151787]
5. Damsky CH, Fitzgerald ML, Fisher SJ. Distribution patterns of extracellular matrix components and adhesion receptors are intricately modulated during first trimester cytotrophoblast differentiation along the invasive pathway, in vivo. J Clin Invest. 1992; 89:210–222. [PubMed: 1370295]
6. Vicovac L, Jones CJ, Aplin JD. Trophoblast differentiation during formation of anchoring villi in a model of the early human placenta in vitro. Placenta. 1995; 16:41–56. [PubMed: 7716127]
7. Fisher SJ, Cui TY, Zhang L, Hartman L, Grahl K, Zhang GY, Tarpey J, Damsky CH. Adhesive and degradative properties of human placental cytotrophoblast cells in vitro. J Cell Biol. 1989; 109:891–902. [PubMed: 2474556]
8. Lala PK, Hamilton GS. Growth factors, proteases and protease inhibitors in the maternal-fetal dialogue. Placenta. 1996; 17:545–555. [PubMed: 8916202]
9. Lee JM, Dedhar S, Kalluri R, Thompson EW. The epithelial-mesenchymal transition: new insights in signaling, development, and disease. J Cell Biol. 2006; 172:973–981. [PubMed: 16567498]
10. Pollheimer J, Loregger T, Sonderegger S, Saleh L, Bauer S, Bilban M, Czerwenka K, Husslein P, Knöfler M. Activation of the canonical wingless/T-cell factor signaling pathway promotes invasive differentiation of human trophoblast. Am J Pathol. 2006; 168:1134–1147. [PubMed: 16565489]
11. Bischof P, Meisser A, Campana A. Paracrine and autocrine regulators of trophoblast invasion—a review. Placenta. 2000; 21(Suppl A):S55–S60. [PubMed: 10831123]
12. Lala PK, Graham CH. Mechanisms of trophoblast invasiveness and their control: the role of proteases and protease inhibitors. Cancer Metastasis Rev. 1990; 9:369–379. [PubMed: 2097085]
13. Loregger T, Pollheimer J, Knöfler M. Regulatory transcription factors controlling function and differentiation of human trophoblast—a review. Placenta. 2003; 24(Suppl A):S104–S110. [PubMed: 12842421]
14. Otterbein LE, Soares MP, Yamashita K, Bach FH. Heme oxygenase-1: unleashing the protective properties of heme. Trends Immunol. 2003; 24:449–455. [PubMed: 12909459]
15. Lyall F, Barber A, Myatt L, Bulmer JN, Robson SC. Hemeoxygenase expression in human placenta and placental bed implies a role in regulation of trophoblast invasion and placental function. FASEB J. 2000; 14:208–219. [PubMed: 10627295]
16. Fournier T, Handschuh K, Tsatsaris V, Evain-Brion D. Involvement of PPARγ in human trophoblast invasion. Placenta. 2007; 28(Suppl A):S76–S81. [PubMed: 17321592]
17. Fournier T, Pavan L, Tarrade A, Schoonjans K, Auwerx J, Rochette-Egly C, Evain-Brion D. The role of PPAR-γ/RXR-α heterodimers in the regulation of human trophoblast invasion. Ann NY Acad Sci. 2002; 973:26–30. [PubMed: 12485829]
18. Kliman HJ, Nestler JE, Sermasi E, Sanger JM, Strauss JF 3rd. Purification, characterization, and *in vitro* differentiation of cytotrophoblasts from human term placentae. Endocrinology. 1986; 118:1567–1582. [PubMed: 3512258]
19. Knöfler M, Saleh L, Bauer S, Galos B, Rotheneder H, Husslein P, Helmer H. Transcriptional regulation of the human chorionic gonadotropin β gene during villous trophoblast differentiation. Endocrinology. 2004; 145:1685–1694. [PubMed: 14715707]
20. Blaschitz A, Weiss U, Dohr G, Desoye G. Antibody reaction patterns in first trimester placenta: implications for trophoblast isolation and purity screening. Placenta. 2000; 21:733–741. [PubMed: 10985978]
21. Strohmer H, Kiss H, Mosl B, Egarter C, Husslein P, Knöfler M. Hypoxia downregulates continuous and interleukin-1-induced expression of human chorionic gonadotropin in choriocarcinoma cells. Placenta. 1997; 18:597–604. [PubMed: 9290157]
22. Graham CH, Hawley TS, Hawley RG, MacDougall JR, Kerbel RS, Khoo N, Lala PK. Establishment and characterization of first trimester human trophoblast cells with extended lifespan. Exp Cell Res. 1993; 206:204–211. [PubMed: 7684692]
23. Genbacev O, Schubach SA, Miller RK. Villous culture of first trimester human placenta—model to study extravillous trophoblast (EVT) differentiation. Placenta. 1992; 13:439–461. [PubMed: 1470605]

Europe PMC Funders Author Manuscripts

24. Bauer S, Pollheimer J, Hartmann J, Husslein P, Aplin JD, Knöfler M. Tumor necrosis factor-α inhibits trophoblast migration through elevation of plasminogen activator inhibitor-1 in first-trimester villous explant cultures. J Clin Endocrinol Metab. 2004; 89:812–822. [PubMed: 14764800]
25. Bilban M, Ghaffari-Tabrizi N, Hintermann E, Bauer S, Molzer S, Zoratti C, Malli R, Sharabi A, Hiden U, Graier W, Knöfler M, Andreae F, Wagner O, Quaranta V, Desoye G. Kisspeptin-10, a KiSS-1/metastin-derived decapeptide, is a physiological invasion inhibitor of primary human tropho-blasts. J Cell Sci. 2004; 117:1319–1328. [PubMed: 15020672]
26. Bilban M, Heintel D, Scharl T, Woelfel T, Auer MM, Porpaczy E, Kainz B, Krober A, Carey VJ, Shehata M, Zielinski C, Pickl W, Stilgenbauer S, Gaiger A, Wagner O, Jager U. Deregulated expression of fat and muscle genes in B-cell chronic lymphocytic leukemia with high lipoprotein lipase expression. Leukemia. 2006; 20:1080–1088. [PubMed: 16617321]
27. Irizarry RA, Bolstad BM, Collin F, Cope LM, Hobbs B, Speed TP. Summaries of Affymetrix GeneChip probe level data. Nucleic Acids Res. 2003; 31:e15. [PubMed: 12582260]
28. Tusher VG, Tibshirani R, Chu G. Significance analysis of microarrays applied to the ionizing radiation response. Proc Natl Acad Sci USA [Erratum (2001) 98:10515]. 2001; 98:5116–5121. [PubMed: 11309499]
29. Subramanian A, Tamayo P, Mootha VK, Mukherjee S, Ebert BL, Gillette MA, Paulovich A, Pomeroy SL, Golub TR, Lander ES, Mesirov JP. Gene set enrichment analysis: a knowledge-based approach for interpreting genome-wide expression profiles. Proc Natl Acad Sci USA. 2005; 102:15545–15550. [PubMed: 16199517]
30. Livak KJ, Schmittgen TD. Analysis of relative gene expression data using real-time quantitative PCR and the 2(-Δ Δ C(T)) method. Methods. 2001; 25:402–408. [PubMed: 11846609]
31. Leisser C, Saleh L, Haider S, Husslein H, Sonderegger S, Knöfler M. Tumour necrosis factor-α impairs chorionic gonadotrophin β-subunit expression and cell fusion of human villous cytotrophoblast. Mol Hum Reprod. 2006; 12:601–609. [PubMed: 16896069]
32. Pollheimer J, Knöfler M. Signalling pathways regulating the invasive differentiation of human trophoblasts: a review. Placenta. 2005; 26(Suppl A):S21–S30. [PubMed: 15837062]
33. Das C, Kumar VS, Gupta S, Kumar S. Network of cytokines, integrins and hormones in human trophoblast cells. J Reprod Immunol. 2002; 53:257–268. [PubMed: 11730921]
34. Deshane J, Chen S, Caballero S, Grochot-Przeczek A, Was H, Li Calzi S, Lach R, Hock TD, Chen B, Hill-Kapturczak N, Siegal GP, Dulak J, Jozkowicz A, Grant MB, Agarwal A. Stromal cell-derived factor 1 promotes angio-genesis via a heme oxygenase 1-dependent mechanism. J Exp Med. 2007; 204:605–618. [PubMed: 17339405]
35. Bilban M, Bach FH, Otterbein SL, Ifedigbo E, de Costa d'Avila J, Esterbauer H, Chin BY, Usheva A, Robson SC, Wagner O, Otterbein LE. Carbon monoxide orchestrates a protective response through PPARγ. Immunity. 2006; 24:601–610. [PubMed: 16713977]
36. Ahmed A, Rahman M, Zhang X, Acevedo CH, Nijjar S, Rushton I, Bussolati B, St John J. Induction of placental heme oxygenase-1 is protective against TNFα-induced cytotoxicity and promotes vessel relaxation. Mol Med. 2000; 6:391–409. [PubMed: 10952020]
37. Bainbridge SA, Farley AE, McLaughlin BE, Graham CH, Marks GS, Nakatsu K, Brien JF, Smith GN. Carbon monoxide decreases perfusion pressure in isolated human placenta. Placenta. 2002; 23:563–569. [PubMed: 12361675]
38. Bainbridge SA, Smith GN. HO in pregnancy. Free Radic Biol Med. 2005; 38:979–988. [PubMed: 15780756]
39. Souza AI, Felkin LE, McCormack AM, Holder A, Barton PJ, Banner NR, Rose ML. Sequential expression of three known protective genes in cardiac biopsies after transplantation. Transplantation. 2005; 79:584–590. [PubMed: 15753848]
40. Woo CH, Massett MP, Shishido T, Itoh S, Ding B, McClain C, Che W, Vulapalli S,R, Yan C, Abe J. ERK5 activation inhibits inflammatory responses via peroxisome proliferator-activated receptor δ (PPARδ) stimulation. J Biol Chem. 2006; 281:32164–32174. [PubMed: 16943204]
41. Schild RL, Sonnenberg-Hirche CM, Schaiff WT, Bildirici I, Nelson DM, Sadovsky Y. The kinase p38 regulates peroxisome proliferator activated receptor-γ in human trophoblasts. Placenta. 2006; 27:191–199. [PubMed: 16338464]

Europe PMC Funders Author Manuscripts

42. Lin Q, Weis S, Yang G, Weng YH, Helston R, Rish K, Smith A, Bordner J, Polte T, Gaunitz F, Dennery PA. Heme oxygenase-1 protein localizes to the nucleus and activates transcription factors important in oxidative stress. J Biol Chem. 2007; 282:20621–20633. [PubMed: 17430897]
43. Hauser S, Adelmant G, Sarraf P, Wright HM, Mueller E, Spiegelman BM. Degradation of the peroxisome proliferator-activated receptor γ is linked to ligand-dependent activation. J Biol Chem. 2000; 275:18527–18533. [PubMed: 10748014]
44. Gelman L, Michalik L, Desvergne B, Wahli W. Kinase signaling cascades that modulate peroxisome proliferator-activated receptors. Curr Opin Cell Biol. 2005; 17:216–222. [PubMed: 15780600]
45. Pascual G, Fong AL, Ogawa S, Gamliel A, Li AC, Perissi V, Rose DW, Willson TM, Rosenfeld MG, Glass CK. A SUMOylation-dependent pathway mediates transrepression of inflammatory response genes by PPAR-γ. Nature. 2005; 437:759–763. [PubMed: 16127449]
46. Maruhashi K, Kasahara Y, Ohta K, Wada T, Ohta K, Nakamura N, Toma T, Koizumi S, Yachie A. Paradoxical enhancement of oxidative cell injury by overexpression of heme oxygenase-1 in an anchorage-dependent cell ECV304. J Cell Biochem. 2004; 93:552–562. [PubMed: 15378604]
47. Soares MP, Seldon MP, Gregoire IP, Vassilevskaia T, Berberat PO, Yu J, Tsui TY, Bach FH. Heme oxygenase-1 modulates the expression of adhesion molecules associated with endothelial cell activation. J Immunol. 2004; 172:3553–3563. [PubMed: 15004156]
48. Wagener FA, da Silva JL, Farley T, de Witte T, Kappas A, Abraham NG. Differential effects of heme oxygenase isoforms on heme mediation of endothelial intracellular adhesion molecule 1 expression. J Pharmacol Exp Ther. 1999; 291:416–423. [PubMed: 10490932]
49. Bussolati B, Ahmed A, Pemberton H, Landis RC, Di Carlo F, Haskard DO, Mason JC. Bifunctional role for VEGF-induced heme oxygenase-1 in vivo: induction of angiogenesis and inhibition of leukocytic infiltration. Blood. 2004; 103:761–766. [PubMed: 14525760]
50. Salinas M, Wang J, Rosa de Sagarra M, Martin D, Rojo AI, Martin-Perez J, Ortiz de Montellano PR, Cuadrado A. Protein kinase Akt/PKB phosphorylates heme oxygenase-1 in vitro and in vivo. FEBS Lett. 2004; 578:90–94. [PubMed: 15581622]
51. Takamiya R, Takahashi M, Park YS, Tawara Y, Fujiwara N, Miyamoto Y, Gu J, Suzuki K, Taniguchi N. Overexpression of mutated Cu, Zn-SOD in neuroblastoma cells results in cytoskeletal change. Am J Physiol Cell Physiol [Erratum (2005) 288:C1461]. 2005; 288:C253–C259. [PubMed: 15456693]
52. Handschuh K, Guibourdenche J, Guesnon M, Laurendeau I, Evain-Brion D, Fournier T. Modulation of PAPP-A expression by PPARγ in human first trimester trophoblast. Placenta. 2006; 27(Suppl A):S127–S134. [PubMed: 16388849]
53. Handschuh K, Guibourdenche J, Tsatsaris V, Guesnon M, Laurendeau I, Evain-Brion D, Fournier T. Human chorionic gonadotropin produced by the invasive trophoblast but not the villous trophoblast promotes cell invasion and is down-regulated by peroxisome proliferator-activated receptor-γ. Endocrinology. 2007; 148:5011–5019. [PubMed: 17628005]
54. Shalom-Barak T, Nicholas JM, Wang Y, Zhang X, Ong ES, Young TH, Gendler SJ, Evans RM, Barak Y. Peroxisome proliferator-activated receptor γ controls Muc1 transcription in trophoblasts. Mol Cell Biol. 2004; 24:10661–10669. [PubMed: 15572671]

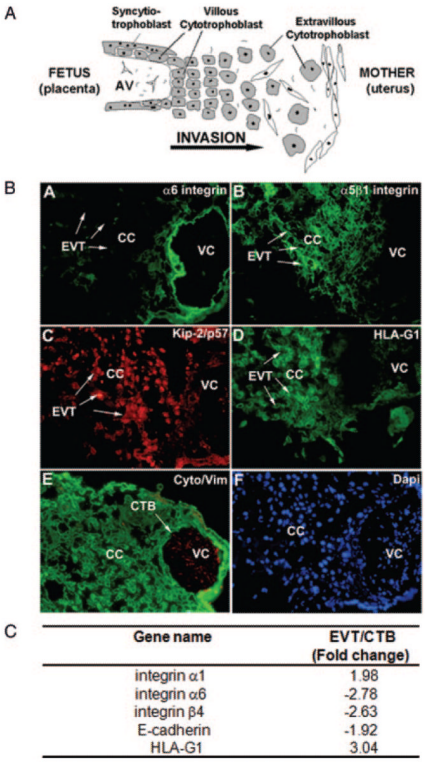

C

Gene name	EVT/CTB (Fold change)
integrin α1	1.98
integrin α6	-2.78
integrin β4	-2.63
E-cadherin	-1.92
HLA-G1	3.04

FIG. 1.

Trophoblast invasion as a model to identify invasion-regulating genes. A, Diagram of the histological organization of the human maternal-fetal interface at early gestation. CTBs, which are specialized (fetal) epithelial cells of the placenta, differentiate into EVTs and invade the uterine wall. EVTs were collected from most distally outgrowing cells of first trimester villous explants growth factor-reduced Matrigel after 72 h culturing, whereas villous CTBs were purified from first trimester placentae as described in *Materials and Methods*. AV, Anchoring villus. B, Localization of integrins α1 and α6, HLA-G1, Kip2/p57, cytokeratin 7 (Cyto) (depicted in *green*), vimentin (Vim) (depicted in *red*) in first trimester villous explant cultures seeded on Matrigel. To visualize nuclei, sections were counterstained with DAPI. The staining pattern is indicative for highly invasive EVTs (marked by *arrows*) or poorly invasive CTBs, respectively. Representative examples are shown. CC, Cell column; VC, villous core. C, GeneChip-derived expression patterns of well-known markers for CTBs and EVTs.

Europe PMC Funders Author Manuscripts
Europe PMC Funders Author Manuscripts

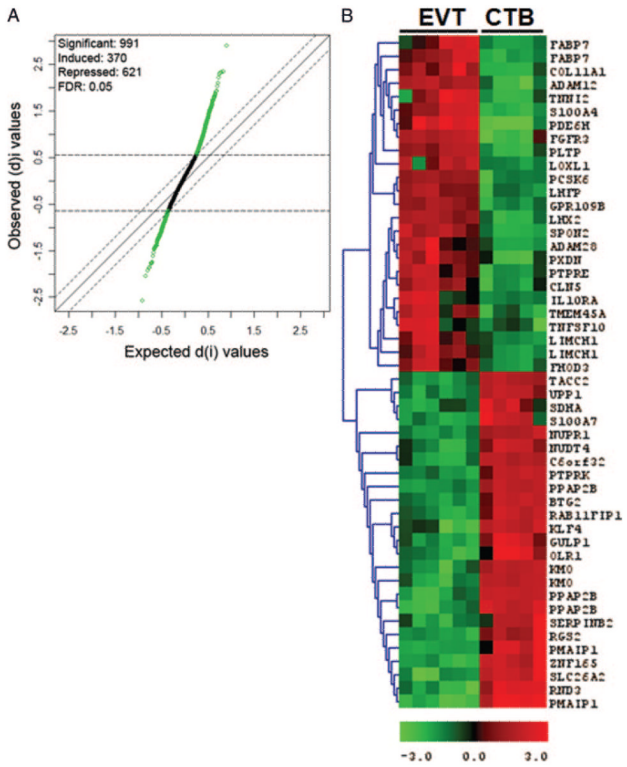

FIG. 2.

Microarray analysis of EVT *vs.* CTB identifies multiple differentially expressed genes. A, SAM analysis between one group of EVT (n = 6) and one group of CTB (n = 5) samples. The scatter plot of the observed difference d(I) *vs.* the expected relative difference $d_E(I)$ is shown. The *broken lines* are drawn at a distance of $\Delta = 0.30$ from the *solid line* that indicates $d(I) = d_E(I)$. Genes outside the *broken lines* are regarded as genes with significant changes in expression, yielding 991 genes. The median estimated FDR is 5%. *Dots above the broken line* indicate genes induced in EVTs (370), and *dots below the broken line* indicate genes that are suppressed in EVTs (621). B, A heat map of top 50 genes that differentiate EVT and CTB groups as judged by SAM analysis. Down-regulated genes are shown in *green* and up-regulated genes in *red*.

Europe PMC Funders Author Manuscripts
Europe PMC Funders Author Manuscripts

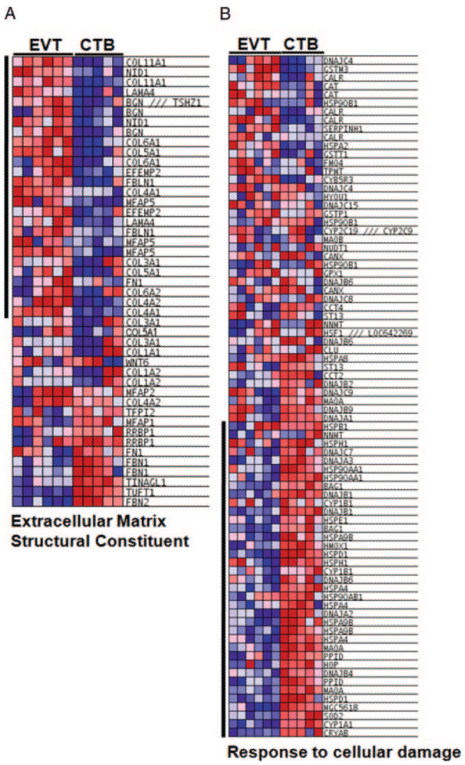

FIG. 3.

Multiple functional gene sets are altered between EVTs and CTBs. Top-scoring pathways displayed as heat maps showing relative gene expression. One exemplary pathway is shown for each category according to Table 3. Down-regulated genes are shown in *blue* and up-regulated genes in *red*. Genes with statistically significant core enrichment are indicated by the *black bar on the left* of the heat maps. A, Example of a top-scoring pathways enriched in EVTs. B, Example of a top-scoring pathways enriched in CTBs.

Europe PMC Funders Author Manuscripts
Europe PMC Funders Author Manuscripts

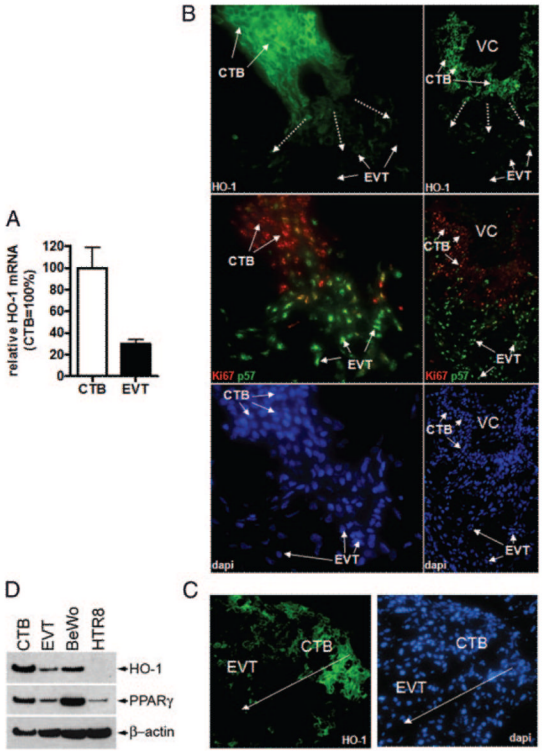

FIG. 4.

HO-1 expression is reduced upon differentiation of CTBs into EVTs. A, Real-time PCR of EVT and CTB mRNAs (each n = 3) was performed as described previously. B, Immunofluorescence of first trimester placental tissues. Two representative examples (*left panel*: 40-fold magnification; *right panel*: 20-fold magnification) of five different placentae analyzed are shown. Serial sections of first trimester placental tissues were incubated with specific antibodies against HO-1 (*upper panels*) and Ki67/Kip2-p57 (*red/green*; *middle panels*) and counterstained with DAPI (*lower panels*). Note that most differentiated, p57-positive EVTs are largely devoid of HO-1. *Dotted line*, Direction of invasion. VC, Villous core. C, Immunofluorescence of tissue sections of first trimester explant cultures seeded on Matrigel (48 h). A representative example of 15 different explants of three different placentae is depicted. *Dotted arrow* denotes direction of trophoblast invasion. D, HO-1 and PPARγ protein expression in primary trophoblast cells and HTR-8/SVneo and BeWo cells. Western blot analysis demonstrated high HO-1 expression in CTB and BeWo and no/low HO-1 protein levels in EVT and HTR-8/SVneo cells, respectively. Note higher PPARγ protein levels in CTBs compared with EVTs. β-Actin was used as a loading ctrl. The *blot* is representative for three independent experiments.

Europe PMC Funders Author Manuscripts
Europe PMC Funders Author Manuscripts

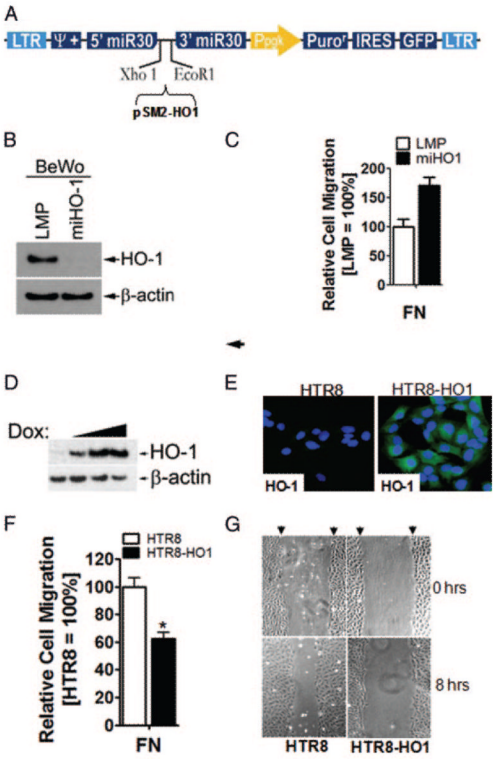

FIG. 5.

HO-1 inhibits trophoblast migration in loss-of as well as in gain-of function cell models. A, A miRNA targeting human HO-1 was shuttled from pSM2 into the retroviral vector LMP used to construct HO-1 knockdown cells as described in *Materials and Methods*. B, Western blot analysis of ctrl (LMP) or HO-1 miRNA-adapted short hairpin RNA transduced BeWo cells (miHO-1) demonstrates efficient HO-1 knockdown. β-Actin indicates equal loading. A representative example is shown. C, Transwell migration assays of LMP and miHO-1 BeWo cells were performed as described in *Materials and Methods*. Cell migration of ctrl-infected cells (LMP) through FN-coated filters was set to 100%. Note that miHO1 cell migration is increased in cells lacking HO-1. D, HTR-8/SVneo cells were retrovirally transduced to express the human HO-1 cDNA under the control of a DOX-sensitive promoter (Tet-On) as described in *Materials and Methods*. HO-1 protein expression in HTR8-HO-1 cells after 24 h DOX addition (0, 0.1, 1.0, and 10.0 μg/ml) was analyzed by Western blotting. β-Actin was used as a loading ctrl. E, Immunofluorescence of mock- or HO-1 transduced cells after 24 h DOX (1 μg/ml) induction using specific HO-1 antibodies. F, Transwell migration assays of DOX-induced HTR8 and HTR8/HO-1 cells were performed as described in *Materials and Methods*. Cell migration of ctrl-infected cells (HTR8) was set to 100%. Note that HTR8/HO1 cell migration through FN-coated filters is reduced in cells expressing HO-1. *Bars* represent mean values ± SEM of three different experiments. *, $P < 0.05$ *vs.* HTR8. G, Effects of HO-1 expression on cell migration in wound healing assays. Wound healing assays of DOX-treated, mock- and HO-1-transduced HTR-8/SVneo cells were performed as described in *Materials and Methods*. Micrographs of wounded, nonfixed cell layers at 0 and 8 h after addition of culture medium are depicted. Initial sizes of wounds are marked by *arrowheads*. Representative examples of three different experiments are shown.

Europe PMC Funders Author Manuscripts
Europe PMC Funders Author Manuscripts

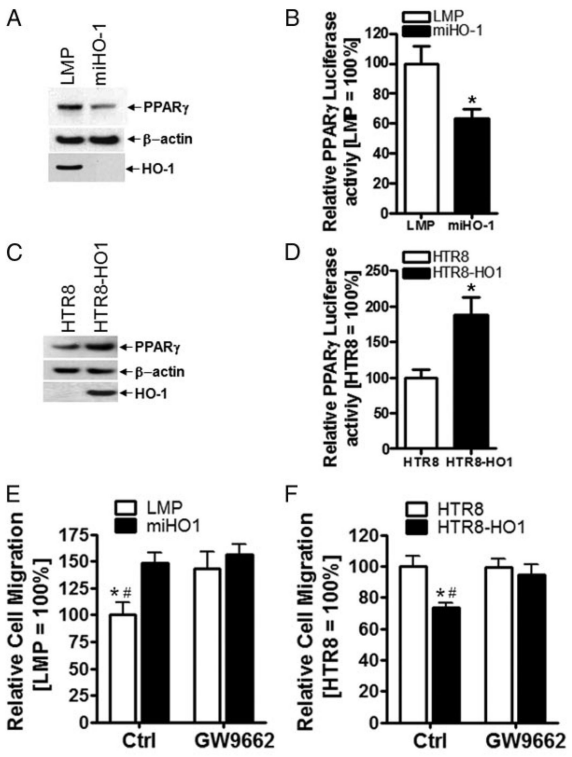

FIG. 6.

HO-1 inhibits trophoblast migration via PPARγ. A, Protein levels of PPARγ were investigated in LMP or miHO1 BeWo cells by Western blotting. HO-1 and β-actin demonstrate HO-1 knockdown with equal protein loading, respectively. Representative examples are shown. B, Luciferase assays of BeWo LMP and miHO-1 cells after cotransfection with PPARγ-responsive and phRL ctrl plasmids. Firefly luciferase activity was determined in protein extracts and normalized to Renilla luciferase activity as described previously. For comparison, values of ctrl (LMP) infected cells were arbitrarily set to 100% in each experiment. *Bars* represent mean values of three independent transfections of three different cultures. *Error bars* indicate SD.*, $P < 0.05$. C, DOX was added to HTR8 and HTR8/HO-1 cells, and PPARγ protein expression was investigated 24–36 h later by Western blotting. HO-1 and β-actin demonstrate increased HO-1 expression with equal protein loading, respectively. D, Luciferase activity of the PPARγ-responsive reporter after 36 h DOX treatment of HTR8 and HTR8/HO-1 cells. Luciferase activity was determined as described in *Materials and Methods*. For comparison, values of ctrl (HTR8) infected cells were arbitrarily set to 100% in each experiment. *Bars* represent mean values of three independent transfections of three different cultures; *error bars* indicate SD.*, $P < 0.05$. E, Transwell migration assays toward FN using LMP or miHO1 cells in the absence (ctrl) or presence of GW9662. Migration of LMP cells was set to 100%. *Bars* represent mean values ± SEM of three different experiments. Note that the inhibitory effect of endogenous HO-1 expression in LMP cells was abrogated when GW9662 was present. *, $P < 0.01$ *vs.* miHO1;#, $P < 0.05$ *vs.* LMP plus GW9662. F, Transwell migration assays of DOX-induced HTR8 and HTR8/HO-1 cells toward FN in the absence (ctrl) or presence of GW9662. Note that the inhibitory effect of HO-1 expression in DOX-treated HTR8/HO-1 cells was abrogated when GW9662 was present. *, $P < 0.05$ *vs.* HTR8;#, $P < 0.05$ *vs.* HTR8/HO-1 plus GW9662.

Europe PMC Funders Author Manuscripts
Europe PMC Funders Author Manuscripts

Europe PMC Funders Author Manuscripts
Europe PMC Funders Author Manuscripts

TABLE 1

Differential mRNA expression of invasion-associated genes in EVT and CTB

GenBank accession no.	Gene name	EVT/CTB GeneChip[a]	EVT/CTB quantitative PCR[b]	*P* value[c]	Left primer (5′–3′)	Right primer (5′–3′)
W46291	ADAM metallopeptidase domain 12	4.20	53.79	0.0003	ACATCAGCAGACCCCTCAAC	AGTGAGCCGAGTTGTTCTGG
NM_021778	ADAM metallopeptidase domain 28	8.33	54.17	0.0052	GCCAGTAGAAGGCAATGAGC	CTCTGCCATCCAGATTTTCC
BF940043	Nidogen 1	5.56	9.04	0.263	AAGATGAATTCCGTGGTTGC	ACTCCCAAGGTGTTGTCAGG
NM_012445	Spondin 2	9.22	38.28	0.0178	ACGGTGACCGAGATAACGTC	GGAACTGAGGCGCTGTCTAC
Y13786	ADAM metallopeptidase domain 19	3.56	12.68	0.0015	TGTGGTAGCTGGAGTGTTGG	TGTTGATCACCTTTCGCTTG
NM_002133	Heme oxygenase 1	−2.02	−3.33	0.0225	CAGGATTTGTCAGAGGCCCTGAAGG	TGTGGTACAGGGAGGCCATCACC
U64317	NEDD9	−5.35	−14.93	0.170	GAGAGGAGCTGGATGGATGA	TCCACGGGCTTTGTAATCTC
AF199015	Villin 2 (ezrin)	−3.60	−10.78	0.0407	GGCTGCAGGACTATGAGGAG	TGGCAGTGTATTCTGCAAGC

[a]F/T: mean fold change of mRNA levels between EVT *vs.* CTB based on GeneChip and real-time PCR, respectively (n = 5 for each group)

[b]F/T: mean fold change of mRNA levels between EVT *vs.* CTB based on GeneChip and real-time PCR, respectively (n = 5 for each group)

[c]Comparison of the mean fold changes of mRNA levels between EVT *vs.* CTB based on real-time PCR

Europe PMC Funders Author Manuscripts
Europe PMC Funders Author Manuscripts

TABLE 2

Top 50 differentially expressed genes between EVTs (n = 6) and CTBs (n = 5)

Representative public identification	Gene symbol	Mean (EVT)	Mean (CTB)	FC (EVT/CTB)	Gene title
NM_006205	PDE6H	1074	33	32.32	Phosphodiesterase 6H, cGMP-specific, cone, γ
NM_002961	S100A4	768	61	12.65	S100 calcium binding protein A4
NM_003282	TNNI2	699	58	11.94	Troponin I type 2 (skeletal, fast)
J04177	COL11A1	445	46	9.78	Collagen, type XI, α 1
W46291	ADAM12	3361	345	9.74	ADAM metallopeptidase domain 12 (meltrin, α)
NM_001446	FABP7	555	59	9.40	Fatty acid binding protein 7, brain
NM_012445	SPON2	1766	191	9.22	Spondin 2, extracellular matrix protein
NM_000142	FGFR3	1135	130	8.72	Fibroblast growth factor receptor 3
NM_001446	FABP7	113	13	8.68	Fatty acid binding protein 7, brain
NM_021778	ADAM28	488	59	8.33	ADAM metallopeptidase domain 28
NM_006227	PLTP	1324	167	7.91	Phospholipid transfer protein
NM_004789	LHX2	318	43	7.44	LIM homeobox 2
NM_018004	TMEM45A	648	89	7.28	Transmembrane protein 45A
NM_001558	IL10RA	516	72	7.19	Interleukin 10 receptor, α
D86983	PXDN	1192	172	6.94	Peroxidasin homolog (*Drosophila*)
NM_005576	LOXL1	755	114	6.60	Lysyl oxidase-like 1
AA775177	PTPRE	637	97	6.59	Protein tyrosine phosphatase, receptor type, E
NM_006493	CLN5	827	134	6.17	Ceroid-lipofuscinosis, neuronal 5
AW474434	TNFSF10	427	70	6.15	TNF (ligand) superfamily, member 10
NM_002570	PCSK6	2713	443	6.13	Proprotein convertase subtilisin/kexin type 6
NM_005780	LHFP	1251	206	6.06	Lipoma HMGIC fusion partner
AK026815	LIMCH1	326	54	6.04	LIM and calponin homology domains 1
NM_006018	GPR109B	1320	219	6.03	G protein-coupled receptor 109B
AB029025	LIMCH1	194	33	5.82	LIM and calponin homology domains 1
NM_025135	FHOD3	366	63	5.82	Formin homology 2 domain containing 3
NM_006997	TACC2	108	814	−7.51	Transforming, acidic coiled-coil containing protein 2
NM_019094	NUDT4	85	652	−7.65	Nudix-type motif 4motif 4 pseudogene 1

Europe PMC Funders Author Manuscripts
Europe PMC Funders Author Manuscripts

Representative public identification	Gene symbol	Mean (EVT)	Mean (CTB)	FC (EVT/CTB)	Gene title
M10098_M	ABHD6	29	227	−7.79	Succinate dehydrogenase complex, subunit A, flavoprotein
NM_015864	C6orf32	154	1212	−7.89	Chromosome 6 open reading frame 32
AF135266	NUPR1	205	1654	−8.08	Nuclear protein 1
NM_003364	UPP1	168	1386	−8.23	Uridine phosphorylase 1
BF514079	KLF4	135	1148	−8.48	Kruppel-like factor 4 (gut)
NM_002844	PTPRK	40	338	−8.50	Protein tyrosine phosphatase, receptor type, K
BC005297	KMO	59	514	−8.69	Kynurenine 3-monooxygenase
NM_006763	BTG2	187	1657	−8.87	BTG family, member 2
NM_025151	RAB11FIP1	53	483	−9.12	RAB11 family interacting protein 1 (class I)
AV725664	PPAP2B	60	566	−9.36	Phosphatidic acid phosphatase type 2B
AI074145	KMO	59	559	−9.41	Kynurenine 3-monooxygenase (kynurenine 3-hydroxylase)
NM_016315	GULP1	61	654	−10.66	GULP, engulfment adaptor PTB domain containing 1
AA628586	PPAP2B	174	2011	−11.58	Phosphatidic acid phosphatase type 2B
NM_002575	SERPINB2	55	652	−11.87	Serpin peptidase inhibitor, clade B, member 2
AB000889	PPAP2B	46	644	−14.12	Phosphatidic acid phosphatase type 2B
AF035776	OLR1	45	646	−14.24	Oxidized low density lipoprotein (lectin-like) receptor 1
BG054844	RND3	98	1704	−17.43	*π*-Family GTPase 3
AI025519	SLC26A2	55	983	−17.86	Solute carrier family 26 (sulfate transporter), member 2
NM_021127	PMAIP1	16	280	−17.95	Phorbol-12-myristate-13-acetate-induced protein 1
NM_003447	ZNF165	36	653	−17.95	Zinc finger protein 165
NM_002963	S100A7	36	670	−18.61	S100 calcium binding protein A7
NM_002923	RGS2	32	709	−22.42	Regulator of G-protein signaling 2, 24 kDa
AI857639	PMAIP1	31	1002	−32.69	Phorbol-12-myristate-13-acetate-induced protein 1

GTPase, Guanosine 5′-triphosphatase

Europe PMC Funders Author Manuscripts
Europe PMC Funders Author Manuscripts

TABLE 3

Pathways enriched in EVTs (n = 6)

Pathway name	Source	Size	NES	NOM p-val	FDR q-val
Extracellular matrix/basement membrane components/motility signaling					
Collagen	GO-0005581	19	2.34	<0.001	0.0005
Fibrillar collagen	GO-0005583	11	2.13	<0.001	0.0081
Extracellular matrix structural constituent	GO-0005201	45	2.06	<0.001	0.0133
Extracellular matrix organization and biogenesis	GO-0030198	12	2.03	<0.001	0.0162
Extracellular matrix (Sensu metazoa)	GO-0005578	110	1.99	<0.001	0.0203
Metalloendopeptidase activity	GO-0004222	41	1.92	<0.001	0.0301
Metallopeptidase activity	GO-0008237	62	1.90	<0.001	0.0323
Basement membrane	GO-0005604	29	1.82	0.0038	0.0546
Cell adhesion	GO-0007155	182	1.82	<0.001	0.0538
Regulation of Wnt receptor signaling pathway	GO-0030111	11	1.98	0.0031	0.0213
Osteogenesis	HUMANPATHS	56	1.53	0.0153	0.1646
G protein-coupled receptor activity	GO-0004930	43	1.65	<0.001	0.1105
Carbohydrate metabolism/energy regulation					
Sugar binding	GO-0005529	40	2.03	<0.001	0.0164
Fructose_and_mannose_metabolism	KEGG	24	2.10	<0.001	0.0095
Growth factor activity	GO-0008083	34	2.16	<0.001	0.0065
Galactose_metabolism	KEGG	18	1.93	<0.001	0.0284
Globoside_metabolism	KEGG	14	1.93	0.0032	0.0281
Sugar porter activity	GO-0005351	14	1.71	0.0181	0.0883
Carbohydrate binding	GO-0030246	76	1.69	<0.001	0.0927
Transport/posttranslational modification activities					
Phosphate transport	GO-0006817	19	2.33	<0.001	0.0009
Transferase activity, transferring hexosyl groups	GO-0016758	52	2.01	<0.001	0.0178
Copper ion binding	GO-0005507	28	2.11	<0.001	0.0087
Peroxidase activity	GO-0004601	11	1.98	<0.001	0.0207
Phosphoric diester hydrolase activity	GO-0008081	13	1.98	0.0031	0.0207
Hydrolase activity, hydrolyzing O-glycosyl compounds	GO-0004553	30	1.81	0.0038	0.0554
Calcium ion homeostasis	GO-0006874	14	1.80	0.0032	0.0586

Europe PMC Funders Author Manuscripts
Europe PMC Funders Author Manuscripts

Pathway name	Source	Size	NES	NOM p-val	FDR q-val
Oxidoreductase activity, acting on paired donors, with incorporation	GO-0016706	10	2.13	<0.001	0.0079
Subtilase activity	GO-0004289	12	2.38	<0.001	0.0004
UDP-glycosyltransferase activity	GO-0008194	38	2.06	<0.001	0.0140

The number of genes contained within one pathway/gene set is given by “Size.” Normalized ES (“NES”) is calculated by the GSEA software. Statistical significance is indicated by the nominal *P* value (“NOMp-val”), and the error is controlled by the FDR (“FDR q-val”). UDP, Uridine 5′-diphosphate

Endocrinology. Author manuscript; available in PMC 2011 March 28.

Europe PMC Funders Author Manuscripts
Europe PMC Funders Author Manuscripts

TABLE 4

Pathways enriched in CTBs (n = 5)

Pathway name	Source	Size	NES	NOM p-val	FDR q-val
Stress response					
Nitric oxide	HUMANPATHS	63	−2.15	<0.001	0.0019
Stress/toxicity pathway finder	HUMANPATHS	67	−1.76	0.0013	0.0549
Stress response to cellular damage	HUMANPATHS	80	−1.71	<0.001	0.0772
Cardiovascular disease	HUMANPATHS	77	−1.71	0.0012	0.0776
Response to unfolded protein	GO-0006986	35	−1.52	0.0243	0.1973
Heme binding	GO-0020037	18	−1.91	<0.001	0.0279
DNA damage signaling pathway	HUMANPATHS	57	−1.66	0.0050	0.1019
Signal transduction regulation					
G protein-coupled receptor signaling	HUMANPATHS	51	−1.64	0.0037	0.1189
cAMP/CA^{2+} signaling pathway finder	HUMANPATHS	50	−1.96	<0.001	0.0699
Glucocorticoid signaling I	HUMANPATHS	52	−1.88	<0.001	0.0279
ATPase activity	GO-0016887	124	−1.86	<0.001	0.0309
GTPase activity	GO-0003924	80	−1.78	0.0012	0.0485
Pyrophosphatase activity	GO-0016462	221	−1.95	<0.001	0.0473
Positive regulation of protein kinase activity	GO-0045860	19	−1.64	0.0155	0.1123
Steroid hormone receptor activity	GO-0003707	21	−1.63	0.0156	0.1242
Gene regulation					
Nuclear import	GO-0051170	62	−1.88	0.0012	0.0270
Pore complex	GO-0046930	54	−1.86	0.0013	0.0295
Protein-nucleus import	GO-0006606	62	−1.85	0.0012	0.0288
Nuclear pore	GO-0005643	54	−1.85	<0.001	0.0282
Nucleoside-triphosphatase activity	GO-0017111	216	−1.93	<0.001	0.0319
RNA splicing	GO-0008380	101	−1.84	<0.001	0.0308
Translation factor activity, nucleic acid binding	GO-0008135	52	−1.83	<0.001	0.0301
mRNA processing	GO-0006397	131	−1.70	<0.001	0.0744
Amino acid and lipid metabolism					
Tryptophan_metabolism	KEGG	37	−1.89	<0.001	0.0283
Glutamate_metabolism	KEGG	21	−1.92	<0.001	0.0294

Europe PMC Funders Author Manuscripts
Europe PMC Funders Author Manuscripts

Pathway name	Source	Size	NES	NOM p-val	FDR q-val
Hydrolase activity, acting on acid anhydrides	GO-0016817	221	−1.94	<0.001	0.0408
Triacylglycerol biosynthesis	BIOCYC	10	−1.77	0.0152	0.0512
Phospholipid_degradation	KEGG	13	−1.69	0.0103	0.0834
Tetrapyrrole binding	GO-0046906	18	−1.93	<0.001	0.0289
Coenzyme biosynthesis	GO-0009108	34	−1.85	0.0027	0.0273

The number of genes contained within one pathway/gene set is given by “Size.” Normalized ES (“NES”) is calculated by the GSEA software. Statistical significance is indicated by the nominal *P* value (“NOMp-val”), and the error is controlled by the FDR (“FDR q-val”). ATPase, Adenosine triphosphatase; GTPase, guanosine 5′-triphosphatase